OPTICAL DIFFRACTION STUDIES OF MUSCLE FIBERS

MASATAKA KAWAI *and* IRWIN D. KUNTZ

From the Departments of Biology and Chemistry, Princeton University, Princeton, New Jersey 08540. Dr. Kawai's present address is the Department of Neurology, College of Physicians and Surgeons of Columbia University, New York 10032. Dr. Kuntz's present address is the Department of Pharmaceutical Chemistry, School of Pharmacy, University of California, San Francisco, California 94122.

ABSTRACT A new technique to monitor light diffraction patterns electrically is applied to frog semitendinosus muscle fibers at various levels of stretch. The intensity of the diffraction lines, sarcomere length change, and the length-dispersion (line width) were calculated by fast analogue circuits and displayed in real time. A helium-neon laser (wavelength 6328 Å) was used as a light source. It was found that the intensity of the first-order diffraction line drops significantly (30–50%) at an optimal sarcomere length of 2.8 μm on isometric tetanic stimulation. Such stimulation produced contraction of half-sarcomeres by about 22 nm presumably by stretching inactive elements such as tendons. The dispersion of the sarcomere lengths is extremely small, and it is proportional to the sarcomere length (less than 4%). The dispersion increases on stimulation. These changes on isometric tetanic stimulation were dependent on sarcomere length. No vibration or oscillation in the averaged length of the sarcomeres was found during isometric tetanus within a resolution of 3 nm; however, our observation of increased length dispersion of the sarcomeres together with detection of the averaged shortening of the sarcomere lengths suggests the presence of asynchronous cyclic motions between thick and thin filaments. An alternative explanation is simply an increase of the length dispersion of sarcomeres without cyclic motions.

INTRODUCTION

Skeletal muscle fibers have very regular cross striations along the fiber axis when examined with light and electron microscopy. They have well-defined alternating A and I bands that have different refractive indices, and the repetitive gradient of the refractive indices causes diffraction effects when the muscle is illuminated by strong beam of light. The appearance of the diffraction patterns projected on a screen is a series of hyperbolic lines with their major axis being the same as that of the fibers (see April et al., 1971; Hill, 1953 *a*; Marikhin and Myasnikova, 1970). The lack of strong, large-scale periodicity on the transverse axis of the muscle results in diffraction *lines* above and below the meridional plane, rather than *spots* of Laue type

(Buchthal and Knappeis, 1940). Thus the diffraction phenomenon in muscle can be approximated by simple diffraction of a one-dimensional grating.

The intensity of the diffraction lines is related to the first several terms in the Fourier transform of optical image, and with intensity and phase data one can, in principle, reconstruct the image of the sarcomeres (Dewey et al., 1972) to a resolution of the wavelength of the light in use. Even in an ideal case one cannot go beyond this limit, and therefore the intensity measurements cannot give much insight on the molecular basis of muscle contraction. Sandow (1936 *a*, *b*) photographically observed intensity changes of the first three orders of diffraction lines of frog sartorius muscles, but he did not derive conclusions. Intensity measurements of the diffraction spectra were repeated by Buchthal and Knappeis (1940) and by Hill (1953 *a*, *b*).

One can measure the length of the sarcomeres (grating spacing) very accurately by optical diffraction technique, making it possible to observe a 50 Å change in the sarcomere lengths using the technique of Cleworth and Edman (1969). This is also true for measurements of the length dispersion of the sarcomeres which can be detected by measuring the width of the diffraction line(s) (Marikhin and Myasnikova, 1970; Kawai, 1971; Dewey et al., 1972). These reports agree that the dispersion of the sarcomere lengths is in the range of 1–5 % in resting muscle fibers. Larson et al. (1968) and Goldspink et al. (1970) detected fluctuations (1.0–1.7 %) of the sarcomere lengths during isometric tetanus of whole frog sartorius muscle and chick latissimus dorsi and they used their observation as evidence for extra energy consumption during isometric tetanus. However, Cleworth and Edman (1969) failed to detect any fluctuational motion of the sarcomeres in frog semitendinosus single muscle fibers, which presumably have a smaller dispersion in the sarcomere lengths than the whole muscles.

In this report, careful studies of the first-order diffraction line on frog semitendinosus muscle fibers are presented, with particular attention paid to the behavior of the length of the sarcomeres in resting muscle fibers as well as isometrically stimulated fibers at various levels of prestretch. Preliminary results on the intensity behavior of the first-order diffraction line are also discussed.

MATERIALS AND METHODS

Dissection of Fibers

Frogs (*Rana pipiens*) were killed by pithing the spinal cords. Semitendinosus muscles were removed with both dorsal and ventral heads attached together, and they were equilibrated in the standard saline consisting of NaCl, 115 mM; KCl, 2.5 mM; $CaCl_2$, 1.8 mM; Na_2HPO_4, 2.15 mM; NaH_2PO_4, 0.85 mM for about 1 h. The same saline was used throughout the dissection as well as the diffraction experiments. The dissection and experimentation were carried out at room temperature, 20–23°C.

A small hole was cut in the tibias tendon by a needle point, and a fishhook of platinum wire was inserted in the hole to permit tension measurements (see below). A Wild dissecting microscope (Wild Heerbrugg Instruments, Inc., Farmingdale, N. Y.) was employed with

magnifications of ×6 to ×50. The ventral head of the muscle was removed as were the exterior fibers of the dorsal head. A particular effort was made to remove innervating tissue. Dissection proceeded until a very small bundle (two to nine fibers) was obtained. The length of tendons was trimmed as short as possible, because elasticity of the tendons influences the time-course of tension greatly. Furthermore, droplets of flexible collodion solubilized in ethanol were applied to the tendon and platinum wire junctions (the tendon was not air dried) in the saline by use of a syringe in order to hold the hook rigidly in place. Without the collodion we always observed delay in tension development. Care must be taken to apply the collodion only to the tendon and platinum wire, because it is harmful to muscle tissue. The saline was replaced many times after collodion application. The dissection was performed in the sample chamber which was made of transparent Lucite and was mounted horizontally on an *X-Y* stage. The experimental set up is shown in Fig. 1.

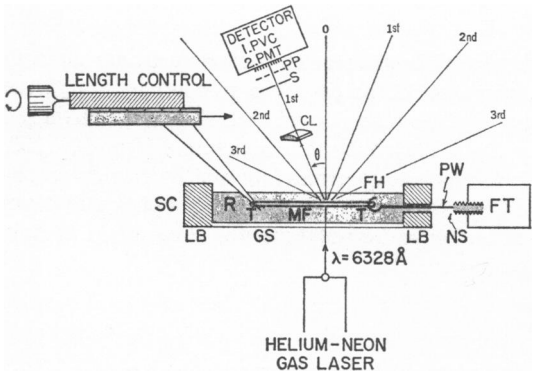

FIGURE 1

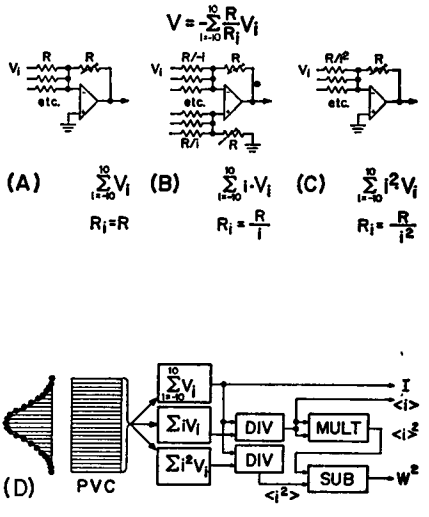

FIGURE 2

FIGURE 1 General outline of the experimental set-up. The laser beam enters into the sample chamber (SC) from the bottom which is made of a glass slide (GS). Then the beam is diffracted by muscle fibers (MF) into individual diffraction orders (0, 1st, 2nd, 3rd, etc.). The detector (PVC array, or PMT) is usually placed on the axis of the first-order diffraction perpendicular to the plane of the drawing (meridional plane). The diffracted beam is focused on the detector by a cylindrical lens (CL). Paraffin paper (PP) is usually placed in front of the detector to avoid the granular nature of the diffraction pattern, and a wide slit (S) is used with the photo tube. The tibias tendon (T) of the fibers is connected to a force transducer (FT) by a fishhook (FH) of a platinum wire (PW) and a nylon screw (NS). The pelvic tendon is connected to a micromanipulator via a forceps and a block of Teflon (not shown) for the length control of the muscle preparation which is soaked in Ringer's solution (R). The sample chamber consists of the glass slide and a Lucite base (LB).

FIGURE 2 (A–C) Circuit diagram for computations in Eq. 1. (A) Simple summation, all $R_i = R$. (B) First moment, $R_i = R/i$. (C) Second moment, $R_i = R/i^2$. The R_i is the ith input resistance, and $i = 0, \pm1, \pm2 \ldots, \pm10$. (D) Block diagram for computation of intensity (I), center of gravity ($<i>$), and line width squared (W^2) from moments as calculated above. See Eq. 2 for comparison. DIV: divider; MULT: multiplier; SUB: subtractor.

Tension Transducer and Its Link to Muscle Fibers

To measure tension signals we used two transducers: F-100 of Bionix (El Cerrito, Calif.) and FT.03C of Grass Instrument Co. (Quincy, Mass.). Five mercury batteries (RM-42R) were used to drive their bridges. Compliance of these transducers is 2 μm/g (F-100) or 25 μm/g (FT.03C).

The fast time-course of tension measurements on muscle fibers required the connecting piece from the muscle to the tension transducer to be as small as possible. In order to reduce the size of this connecting piece, a small hole (about 1 mm in diameter) was cut in one end of the chamber allowing a thin platinum wire to pass from the fiber to transducer. Although this hole was below the level of the saline in the chamber, the hole was small enough to permit surface tension to keep it sealed. The tension transducer was mounted just outside of this hole. The platinum wire had a very small fishhook to hold the tibias tendon of the semitendinosus fibers, and the other end of the wire was attached, by a small amount of epoxy, to a nylon screw through a hole that was drilled into the screw. The nylon screw helps to insulate the platinum wire, which is soaked in the saline, from the external case of the transducer (Fig. 1, NS). The net weight of the wire and the screw was about 0.1 g. The length of the muscle fibers could be adjusted by a micromanipulator which was hooked to the pelvic tendon by insulated forceps.

Stimulus

Electric DC pulses were applied through a pair of bright platinum wire electrodes on both sides of the muscle fibers (10 mm apart, about 50 kΩ across when measured through the saline). A train of pulses was generated in a digital circuit network which was synchronized to the recording system. The control pulses drove Tektronix pulse generators (type 162, 163, Tektronix, Inc., Beaverton, Ore.) for width and height controls, followed by current amplification by a Sorensen power supply (model QRD 60-1.5, Sorensen Power Supplies, Raytheon Co., Manchester, N. H.). A train of 10–50 pulses in 200–500 ms was used as the tetanic stimulation. Each output pulse was 24 V and lasted 100 μs.

Laser

We used a Spectra-Physics model 130C, helium neon laser with a wavelength of 6,328 Å (Spectra-Physics, Inc., Mountain View, Calif.). The beam dimension was 2 mm and it is well collimated. The nominal intensity was 2 mW. There is considerable 120 Hz modulation of the laser intensity (5%). Because of the low diffracting ability of fibers, we sometimes used a cylindrical lens (f2.5) between the sample and detector to focus the diffracted line on the meridional plane.

To control the position of the sample fibers relative to the laser, the chamber, the micromanipulator control for the muscle length, and the tension transducer were mounted on the *X-Y* stage which could be positioned to $\pm$0.1 mm with respect to the laser beam. Care was taken to avoid optical signals from the portion of the fibers near the neuromuscular junction.

Detection

To detect various portions of the diffracted light we employed two different methods. Intensity measurements were primarily made with a conventional 2 inch end-window photomultiplier tube (PMT, e.g. no. 6292, Fairchild Systems Technology Div., Fairchild Camera & Instrument Corp., Palo Alto, Calif.). Intensity data, as well as the average sarcomere length and line width of the diffraction pattern, could be obtained using an array of silicon photo-

voltaic cells (PVC). Most of our experiments were performed using an array of 20 cells with array dimensions of 20 × 20 mm (available on special order from Centralab, El Monte, Calif). The intensity, gain, and noise level of these units were tested and the best ones were selected. Each PVC in the array was connected to a high impedance amplifier (Philbrick/Nexus 1009, Philbrick/Nexus Research, Boston, Mass.). Gain and base-line adjustment could be made independently.

The array was ordinarily positioned on the meridional plane with the first-order diffraction line approximately centered on the middle elements of the array. The distance from the sample to the detector was chosen such that there were a few "base-line" channels at the ends of the array, before, during, and after stimulation. Background scattering was subtracted from diffracted light electrically using the base-line channels before stimulation as "zero." The 20 outputs from the PVC array were monitored by using a multiplexer circuit and were displayed on an oscilloscope. The intensity distribution for each diffraction line was roughly gaussian. We can extract from such a distribution, (*a*) the area under the curve (intensity), (*b*) the center of gravity (position relative to the center of the PVC array), and (*c*) the line width of the distribution. These parameters were calculated "on-line" with fast analogue circuits (Fig. 2) and were recorded in a CAT computer. The tension signal was simultaneously recorded. Details of the detection system and experimental set-up were described previously (Kawai, 1971).

Data Analysis

The analogue circuits and computations will be described in some detail. Essentially we compute for a single diffraction line the zero, first, and second moments of the intensity distribution (Eqs. 1 *a*, *b*, *c*). Then in the usual way, we calculate the area, center of gravity, and line width from these moments (Eqs. 2 *a*, *b*, *c*).

$$M_0 = \sum_{i=1}^{20} V_i , \tag{1a}$$

$$M_1 = \sum_{i=1}^{20} i \cdot V_i , \tag{1b}$$

$$M_2 = \sum_{i=1}^{20} i^2 \cdot V_i , \tag{1c}$$

where V_i is an output of ith PVC, and the summations are taken over 20 PVC channels. The intensity of the diffraction line I, the center of gravity $< i >$, and the line width W are calculated as follows (Eqs. 2 *a*, *b*, *c*):

$$I = M_0 \tag{2a}$$

$$<i> = M_1/M_0 \tag{2b}$$

$$W = 2[(M_2/M_0) - (M_1/M_0)^2]^{1/2} \tag{2c}$$

The Eqs. 2 *a*, *b*, *c* are represented in PVC channel units. In order to convert these parameters into actual distances in sarcomere length, one has to multiply Eqs. 2 *b*, *c* by $|\delta S/\delta x|d$,[1] where d is the width of each photo cell (d = 1 mm).

[1] By differentiation of the grating equation (Eq. 18: $n\lambda = S \sin \theta$) with respect to S and θ one gets

Our basic computational unit is an operational amplifier in a "weighted adder" configuration (Figs. 2 A–C). As shown in this figure, M_0 is a simple summation of V_i (Fig. 2 A). To calculate M_1 one can adjust the input resistances to be reciprocally proportional to the channel number i ($i = 1, 2, 3, \cdots, 20$, or $i = 0, \pm1, \pm2, \cdots, \pm10$) as shown in Fig. 2 B. Similarly, the input resistances are reciprocally proportional to i^2 to get M_2 (Fig. 2 C). To obtain parameters in Eqs. 2 *b*, *c*, two analogue dividers (model D401, Intronics Inc., Newton, Mass.) and a multiplier (M401) were used. The block diagram is shown in Fig. 2 D. We actually calculated the square of W, but for small changes $\delta(W^2) \simeq 2\,W \cdot \delta W$. The limiting precision was 5% in intensity (because of 120 Hz modulation on the laser), ±3 nm in sarcomere length[2] and ±10 nm in its dispersion[3] at typical sarcomere lengths of 2.5 μm using the first-order diffraction line at 50 cm from the muscle fibers.

RESULTS

Fiber Quality

One of our first concerns was to develop some criteria for fiber quality. The major test was to measure the length-tension relationship (Gordon et al., 1966 *b*), which was carried out simultaneously with the diffraction experiments. In all the data in this report, the length-tension plot exhibited a plateau at 2.0–2.3 μm of sarcomere length, then decreased linearly, approaching zero as the sarcomere length reached 3.6 μm. If the plot deviated greatly from this standard the optical data were not used. The bad preparations usually showed a wide range of sarcomere lengths (Fig. 3 B). Fiber bundles of good quality showed quite constant sarcomere length along the length of the fibers (Figs. 3 A, C). Damaged preparations also slowed multiple contractions on a twitch stimulus, unusual deflection points in the length-tension plot, etc.

Diffraction Results

Static Measurements. (*a*) *Intensity measurements.* The intensity of the first-order diffraction line was measured from a bundle of several fibers with the PMT. The PMT was placed 40 cm from the sample, and a slit of 35 mm was placed in front of the PMT. The position of the PMT was adjusted so that the center of the first-

$$\delta S = -\frac{(S^2 - n^2\lambda^2)^{3/2}}{Sn\lambda} \cdot \frac{\delta x}{l} \qquad (3)$$

where S is the sarcomere length; n is the order of the diffraction line; λ is the wavelength of the laser beam (0.6328 μm); l is the distance from fiber to detector; $x = l \cdot \tan\theta$; θ is the angular separation of the nth order line from zero-order reference.

[2] We measure only the absolute position of the first-order diffraction line. Sarcomere length is related to the separation of the zero- and first-order lines. Independent experiments showed that careful orientation of the fiber bundle with respect to the laser beam was sufficient to guarantee no motion of the zero-order line during stimulation.

[3] The observed width of the diffraction line arises from several factors including: "natural" dispersion of sarcomere length in addition to optical "artifacts" such as the finite width of the laser beam, thickness of the fibers, lens imperfections, detector uncertainty, etc. See Appendix I.

order diffraction line always fell on the center of the PMT at each sarcomere length. The cylindrical lens was used, and a sheet of paraffin paper was placed in front of the PMT to scatter the diffracted light to reduce position-dependent sensitivity differences on the photocathode of the PMT.

When the first-order diffraction intensity was measured along the length of the fibers, the photocurrent output usually differed as much as three times in comparing one end of the fiber bundle with the other. A major source of this intensity variation is possibly due to the interference from the small amounts of nerve tissue. It is also possible that the thickness and width of the fibers change. Such a large difference in diffracted light intensity indicates the necessity of examining the same portion of the muscle fibers when their length is changed. Thus we fixed the portion of the muscle fibers illuminated by laser beam and measured the first-order resting intensity vs. sarcomere length (Fig. 7). The PMT output was observed to increase monotonically when the bundle was stretched at a constant slit width (35 mm). The measurements were repeated three times and the result was quite reproducible. However, the measurement must be modified so that the PMT collects only the light of the first-order diffraction line. This cannot be done at a constant slit width, because the angular domain of the first-order diffraction line lessens as the sarcomere length increases. Therefore one has to use a narrower slit at a higher sarcomere length. The width of the slit can be calculated by Eq. 3. If it is 35 mm at $S = 2.6$ μm, it must be 24 mm at $S = 3.8$ μm. When this new slit was used at 3.8 μm the intensity of the first-order line dropped to the level of lower sarcomere length as shown by the arrow in Fig. 4. Since both Eq. 3 and data points in Fig. 4 are monotonic functions of S, one can conclude that the intensity of the first-order diffraction line is essentialy independent of the sarcomere length. This is a difficult measurement, and we should not place heavy reliance upon it, but its theoretical significance is that the amplitude of the first Fourier coefficient is independent of the sarcomere length in the range 2.6 to 3.8 μm (see Appendix II).

(*b*) *Sarcomere length variation along the fibers.* The sarcomere length variation along the fibers was measured when the sarcomere length of the center of the fibers was 2.5 or 3.5 μm (Fig. 3 A, C). S varied by about ± 1 % over the measurable region of the fibers.[4] Poor fibers show sarcomere length variation as large as 20% (Fig. 3 B). In addition we observed that the sarcomere length (in the range of 2.1–3.6 μm) is linearly related to the degree of passive stretch of the fibers as measured by micromanipulator. The result is slightly different from Sandow's (1936 *a*) observation that the plot deviates from linearity when the sarcomere length is less than 2.47 μm in whole sartorius muscle. In semitendinosus fibers, we find that the passive stretch

[4] Note that our experiments do not measure the extreme ends of the fibers because of the 2 mm diameter of the laser spot. This explains why we did not observe shorter sarcomeres at the extreme ends of the fibers, and our results do not contradict the general observation that sarcomeres are shorter in the terminal 0.5 mm of frog semitendinosus fibers (Carlsen et al., 1961; Huxley and Peachey 1961; Gordon et al., 1966 *a*).

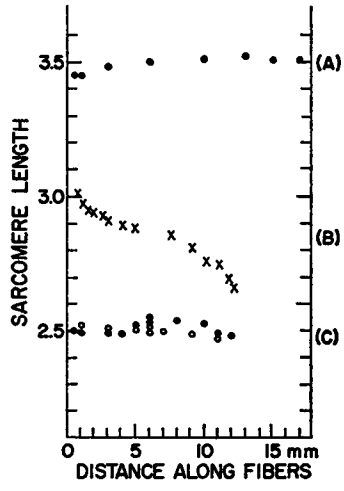

FIGURE 3 Variation of the sarcomere length along the axis of the muscle fibers. A and C are plots of the same bundle of two fibers of high quality at two different sarcomere lengths. Closed and open circles in C are before and after a 3 h experiment, respectively, and crosses in B were obtained from a different preparation of poor quality.

distributes homogeneously along the fibers. The slope of the plot of passive stretch vs. sarcomere length gives the number of sarcomeres along the fiber axis. This can be used to give an accurate estimate of the fiber length.

(*c*) *Length dispersion of sarcomeres vs. sarcomere length.* As indicated above, the observed line width of the first-order diffraction line is made up of an intrinsic dispersion of the lengths of the sarcomeres and a contribution from the finite size of the laser beam. The separation of these terms is developed in Appendix I. The following remarks refer only to the *intrinsic* dispersion in the lengths of the sarcomeres.

We find that the dispersion (line width) is proportional to the sarcomere length for passive stretching and is, on average, about 1–2% of the sarcomere length (exp. no. 660–686 in Table I). The dispersion considerably increases after vigorous stimulation of the fibers, approaching 3–4% of the sarcomere length (exp. no. 497, 652 in Table I). In whole sartorius muscle the dispersion is found to be 10% or more. The above numbers agree well with the observation of the sarcomere length distortion (1.3–3%) by Marikhin and Myasnikova (1970) on frog ileofibularis muscle fibers at one fixed sarcomere length (2.75 μm). They excluded the effect of finite size of laser beam by measuring widths of the higher order diffraction lines. Dewey et al. (1972) also report that the variation in sarcomere lengths in glycerinated *Limulus polyphemus* single fibers is usually less than 5% for sarcomere lengths of 5–10 μm.

Dynamic Properties of the Diffraction Patterns. Using the PVC array and the analogue circuits previously described, we measured the changes in the intensity, center of gravity, and line width of the first-order diffraction line during isometric

TABLE I

RESULTS OF THE MEASUREMENTS OF THE SARCOMERE LENGTH DISPERSION

exp. no.	Number of fibers in a bundle	Sarcomere length (S)	Distance of observation	Dispersion of sarcomere length ($\%S$)*	Number of data points
		μm	cm		
497	7	2.2–3.6	50	3.62 ± 0.36	9
652	2	2.1–3.6	48–49	3.39 ± 0.14	16
660–662	5	2.4–3.8	42–116	0.75 ± 0.27	29
671–673	9	2.8–3.4	34–110	1.96 ± 0.22	22
680–686	11	2.5–4.3	44–122	2.33 ± 0.34	45

* $(2/S_0)\ [\overline{(S - S_0)^2}]^{1/2}$ is shown with standard deviation. Note that fibers in the first two columns experienced stimulation, whereas fibers in the last three columns did not experience any stimulation before the width measurements.

tetanic contraction. We first describe the steady-state effects occurring during the plateau of tension. In general we found a marked decrease (30–50%) in first- and second-order intensity, a small (1%) contraction of the sarcomere length, and an increase of the length dispersion of the sarcomeres to about twice its initial value. These changes were reproducible for any one fiber bundle throughout a 2–3 h experiment. The effects were marked in the center of the fibers and were generally small at the ends of the fibers.

We investigated the sarcomere length dependence for the optical signals (Fig. 4). As expected from the tension work, the changes of the intensity of the first-order diffraction line (ΔI), the sarcomere length (ΔS), and its dispersion (ΔW) approached zero when the fibers were stretched to $S = 3.5$–3.6 μm. The appearance of these plots is, however, very different from that of length-tension relation in which tension declines linearly in this sarcomere length (2.2–3.6 μm) range (Gordon et al., 1966 *b*). The most striking feature of the intensity plot (Fig. 4 A) is that the intensity change is maximum near $S = 2.8$ μm, and it becomes progressively smaller at either shorter and longer lengths of sarcomeres and becomes zero at $S = 2.1$ μm or $S = 3.5$ μm. This tendency was also confirmed by use of a PMT to obtain less noisy data (Fig. 4 B). Changes as large as 30–50% in the intensity of the first-order diffraction line are remarkable, because the total length of the fibers is conserved and so is the local sarcomere length as judged from Fig. 4 C. Indeed the maximum change of the sarcomere length was only 44 nm, that is, about 1.5% of the sarcomere length.

The magnitude of the sarcomere length change (ΔS) increased when the length (S) increased from 2.2 to 2.6 μm, then exhibited a plateau value of 44 nm in the range of $2.6\ \mu m \leq S \leq 3.2\ \mu m$, and decreased linearly to zero again if $3.2\ \mu m \leq S \leq 3.6\ \mu m$ (Fig. 4 C). The data for the length dispersion change (ΔW) are much more scattered (Fig. 4 D, as shown in $\%S$), but one can conclude from this result that the magnitude of the length dispersion change decreases monotonically from

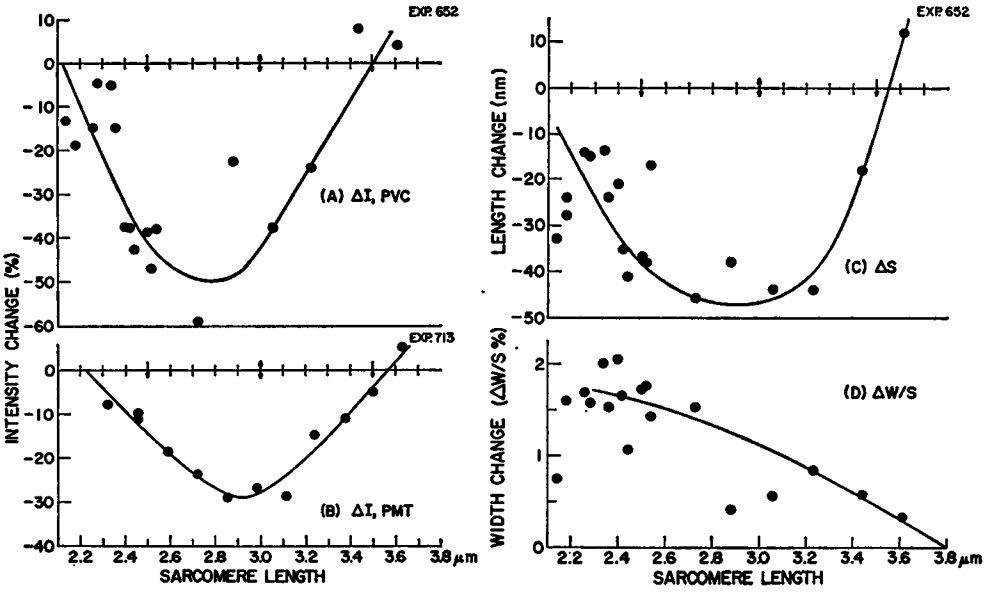

FIGURE 4 Changes in optical signals with sarcomere length. Magnitudes were obtained from the plateau of isometric tetanic contraction. (A) and (B): intensity change of the first-order diffraction line. (A) Measured with PVC, (B) with PMT (different preparations). (C) Change in sarcomere length. (D) Change in dispersion of the sarcomere length as a fraction of the sarcomere length. An indication of the accuracy may be given by the divergence of the data points. A, C, D are simultaneous measurements on a bundle of two fibers which showed a nice length-tension diagram (a plateau peak at 2.0–2.3 μm of sarcomere length, then decreasing linearly to zero by 3.6 μm). Positive numbers indicate increase of the signal, and negative numbers a decrease.

1.7% at S_i = 2.4 μm to zero at S = 3.8 μm where thick and thin filaments no longer overlap. The behavior of the ΔW at short sarcomere lengths (under 2.4 μm) is not clearly defined in the present experiments.

Because of conflicting earlier reports, we paid particular attention to oscillatory changes in sarcomere length during isometric tetanus. No fluctuation of the sarcomere length during the plateau of the tension was observed within a resolution of 3 nm as shown in trace S in Fig. 5. This agrees with the observation by Cleworth and Edman (1969) on frog semitendinosus muscle fibers and does not coincide with that of Larson et al. (1968) on frog sartorius muscle or Goldspink et al. (1970) on chick latissimum dorsi muscle. The whole muscle is not a good preparation for this experiment since the length dispersion of the sarcomeres in whole muscle is as large as 10% of S (see also Cleworth and Edman, 1969). Heterogeneity of the whole sartorius was also reported by Sandow (1936 *b*) who detected both shortening and lengthening sarcomeres depending on which portion of the muscle he examined. Thus one can detect local activities of the whole muscle by diffraction techniques,

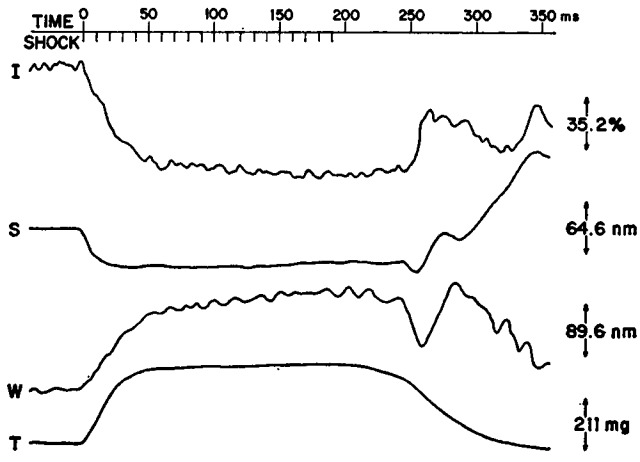

FIGURE 5 Kinetics of optical transients and tension development. Time scale in milliseconds after onset of stimulus. Upward deflection of the signals indicates increase, and downward decrease. *I*, Intensity of the first-order diffraction line; *S*, sarcomere length (resting value was 2.5 μm); *W*, the dispersion of the sarcomere length; *T*, tension. Each trace shows change from the starting value. 60 and 120 Hz ripple is apparent in *W* and *I* traces, respectively.

but the resulting data may not be easy to interpret. The dispersion of the sarcomere length did not fluctuate within a resolution of 20 nm (trace *W* in Fig. 5).[5]

Postcontraction Effects. Changes in the optical diffraction pattern persisted well after the tension declined. As shown in Fig. 5, a big deflection of the optical signals occurred after more than 90% of the tension had been lost. This phenomenon was usually accompanied by a sudden and further reduction in the first-order line intensity, further shortening of the sarcomeres, and further increasing of the length dispersion although it is not very apparent in Fig. 5. Cleworth and Edman (1969) and Huxley and Simmons (1970) reported a local shortening of sarcomeres on the frog semitendinosus single muscle fibers after the bulk of tension had declined. In our diffraction experiments this change started immediately after the tension began to decline, reaching a maximum at about 100 ms afterwards. This phenomenon was reproduced in every preparation, and it tends to become more evident as sarcomere length becomes shorter. Since the magnitude of the signals varied depending on the position of the laser spot along the fibers, it is probably due to unsynchronization of the contractile elements during the decline of tension. For example if some elements lose their activity while others are still active, it could cause a stretching of inactivated elements and a further contraction of the active

[5] When the sarcomeres were stretched to ≥ 3.4 μm, the intensity signal showed some asynchronous oscillation with an amplitude of 20–30% of the resting intensity and a frequency of about 20 Hz. This occurred during the time when tension would reach its plateau value if the sarcomere length were smaller. We have no simple explanation of this phenomenon, but it is definitely different from the fluctuation of the sarcomere length described by Larson and Goldspink and co-workers.

ones. In twitch experiments we often observed nonreproducibility of the signals when we changed the spot of the laser beam along the fiber length, and this is due to the same post contraction effects.

DISCUSSION

Intensity Effects

The intensity of the diffraction pattern should, in principle, represent the first several terms in the Fourier transform of the optical image (see Appendix II). With accurate intensity and phase data one should be able to reconstruct the three-dimensional optical image of the sarcomeres to a resolution of $\sim S/n$ where n is the highest observed diffraction order; $n = 3$ or 4 in the best patterns we have seen and we did not try to synthesize the Fourier series, because n is not big enough for a reasonable estimation of the optical image. The basic diffracting units are thus a large scale (thousands of angstroms) index of refraction gradients presumably associated with the optical elements such as the A, H, M, I, and Z regions of the sarcomeres. The transient change in the diffraction pattern during contraction would then be associated with transient structural changes related to tension development. Thus our observation (Fig. 7) that the intensity of the first-order line is roughly independent of the sarcomere length when the fiber is at rest is not unexpected (see Eq. 19). The contraction machinery is unaltered in a dimension of thousands of angstroms during passive stretching or releasing of the length of the fibers when $S \geq 2.2$ μm, except for the extent of overlap between thick and thin filaments. On the other hand, our observation of very substantial loss of intensity in the first- and second-order lines during tetanic contraction is surprising because, if correct, it implies a substantial structural alteration in quite large structural elements.

There is a variety of possible explanations for the intensity changes. We will discuss these briefly but final resolution of the problem requires further experimentation. We will consider the following explanations: (*a*) loss of registration (disordering) of sarcomeres; (*b*) changes in interfibril spacing; (*c*) multiple diffraction effects; (*d*) scattering effects; and (*e*) changes in index of refraction gradients.

Disordering of Sarcomere Lengths during Contraction. The diffraction pattern contains information about the periodicity both along the muscle fibers and perpendicular to the fibers. Careful alignment of the fibers normal to the laser beam is sufficient for the two spatial dimensions to be orthogonal in the diffraction pattern. That is, the diffraction intensity along the meridional line should contain only information about the one-dimensional periodicity of sarcomeres along the fiber axis. A transverse periodicity of sarcomeres in neighboring fibrils would be reflected in the diffraction pattern above and below the meridional line. In this sense the diffraction pattern is different from the optical image where loss of vertical periodicity is immediately apparent. Our results indicate a general loss of diffraction

intensity both in and out of the meridional plane *without* a major increase in the line width of the diffraction lines. Under isometric conditions the line width measurements during tetanus suggest an increase of the length dispersion of the sarcomeres of order of a few hundred angstroms which should not be sufficient to generate the large intensity loss.

Interfibril Spacings. The interfibril spacings are represented in the broad bands of intensity perpendicular to the meridional plane. Only 10% or so of this light is collected without our one-dimensional lens whereas perhaps 50% is collected with the lens in place. Similar losses of diffraction intensity were recorded with or without the lens thus indicating no preferential loss of intensity above and below the meridional plane.[6]

Multiple Diffraction Effects. The importance of multiple diffraction was considered by Buchthal and Knappeis (1940) and extensively discussed by Hill (1953 *b*). According to Hill, multiple diffraction is significant in a whole muscle such as frog sartorius whose thickness is about eight layers of fibers. In this case, more light is scattered into the higher diffraction orders showing comparable brightness in the zero-, first-, second-, and third-order diffraction lines. Multiple diffraction becomes less important as the number of layers of fibers decreases, and in the case of single fibers or small fiber bundles, like those used in the present experiments the multiple diffraction is negligible. For single fibers, the relative intensity in the higher diffraction orders is much reduced for static intensity measurements (Buchthal and Knappeis, 1940). Furthermore, multiple diffraction effects are strongly linked to the geometry of the diffraction system which is not changing appreciably during isometric contraction (i.e., no rotation of fiber bundles, no significant shortening and thickening of the fibers). Thus the multiple diffraction cannot cause appreciable loss of diffracted intensity on tetanic stimulation under the present experimental conditions. Hill (1953 *b*) briefly noted that the intensities of all the orders of diffraction spectra showed a marked decrease on tetanic stimulation for frog sternocutaneous muscles whose thickness is two to three layers of fibers. On the other hand he did not detect loss of intensity in whole sartorius muscles because of the multiple diffraction effects.

Scattering Effects. From Hill's early work (Hill, 1949) and a recent paper (Barry and Carnay, 1969) it is clear that increases in light scattering *are* associated with changes in activation of muscle and membrane systems. We, too, can clearly see a marked increase in the scattered light during tetanus. Both reports agree that loss of intensity at the peak of the twitch is 2–2.5% in red light (Hill, 1:50

[6] In fact, because the muscle fibers act approximately as a constant volume system, one expects a slight expansion of the fibril spacings on contraction, leading to a somewhat more compact diffraction pattern (the intensity then should *increase* slightly when using a constant solid angle detector). However, this effect is negligible since the shortening of the sarcomere length is only 1.5% or less as judged from Fig. 4 C.

at red light; Barry and Carnay, 2.5% from their Fig. 2 D at 5,500 Å). In tetanus this number approximately doubles. Hence, changes in scattering would appear to be too small to explain the big loss of intensity from the first- and second-order diffraction lines. We do not mean to imply that the increased light scattering is an independent physical event from the intensity effects. It is reasonable to assume that the change in scattering and the change in diffracting ability are both dependent on some internal rearrangements.

Changes in Index of Refraction Gradients. These are clearly the most interesting set of explanations and are mentioned by Huxley (1957). The information of a refractive index difference in sarcoplasm and myoplasm is found in the wide lateral spread of each diffraction line. Since the spacing distribution is irregular the diffraction pattern results in wide lateral spread of intensity rather than discrete spots. On the other hand, the presence of very regular refractive index differences in A band and I band results in several diffraction lines on the meridional plane. Any agitation of the refractive index differences in both transverse and longitudinal directions of the muscle fibers would result in changes of the diffracted light intensity. However, in order to produce the large intensity change we have observed, a severe, large-scale change in the contractile apparatus would be necessary because the local refractive index is a direct function of local protein concentration. As reported elsewhere, translocation of water during contraction may be an important factor but this is not clear as yet. Birefringence of dry myosin fibers was measured by Colby (1971) and it is $10.1 \pm 1.4 \times 10^{-3}$. It decreases by 9% during isometric tetanus (Eberstein and Rosenfalk, 1963) thus yielding a change of only 0.001 refractive index unit. This is probably too small to explain the loss of diffracted light intensity. We are now exploring the possibility that membrane-related conformational changes are significant factors. As indicated at the beginning of this discussion we do not feel a satisfactory explanation of the intensity effects now at hand. We hope that future experiments will solve this problem.

Sarcomere Length and Its Distribution

Resting State. On passive stretching the sarcomere length showed a good linear relationship to the degree of stretch applied by the micromanipulator to the semitendinosus muscle fibers (if $S > 2.1$ μm). This result compares with Sandow's (1936 *a*) observation on sartorius muscle that the sarcomere length is proportional to muscle length if $S \geq 2.47$ μm, but it deviates from proportionality if $S < 2.47$ μm. Thus we can conclude that the stretching by micromanipulator is distributed homogeneously to every sarcomere in the semitendinosus fibers.

Present measurements of the length dispersion of the sarcomeres require several assumptions (Appendix I). They are (*a*) gaussian distribution of the sarcomere lengths, (*b*) incident laser beam intensity is a gaussian distribution, and (*c*) length dispersion is directly proportional to the sarcomere length itself. Among these

assumptions we have to accept the first a priori. There is some question in *b*, because a box or a trapezoid function approximation could be a better representation of the divergence of the laser beam. The linearity of the plot in Fig. 6 proves that the assumption *c* is correct. Marikhin and Myasnikova (1970) report that the dispersion of the sarcomere lengths in frog ileofibularis muscle fibers is 1.3–3 % at one fixed sarcomere length (2.75 μm). They separated out the effect of the finite size of the laser beam by measuring the width of higher diffraction orders. The close correlation between their number and our number (1–2 % for fresh fibers and up to 3.6 % for fibers which experienced electric stimulation) indicates the validity of the assumption *b*. If any errors exist in the estimation of the laser intensity function, they would be a minor correction. However we could not obtain a constant *r* value in Eq. 14 by measuring the slope of the plot. It was somewhat variable between 1.7–3.0 mm. One explanation is that assumption *b* is imperfect, but it is also true that other contributions may change from measurement to measurement. Terms contributing to *r* (optical artifact) are (*i*) finite size of the laser beam, (*ii*) uncertainty associated with the detector because of the discrete point approximation of the continuous diffraction intensity distribution, and the presence of paraffin paper in front of the

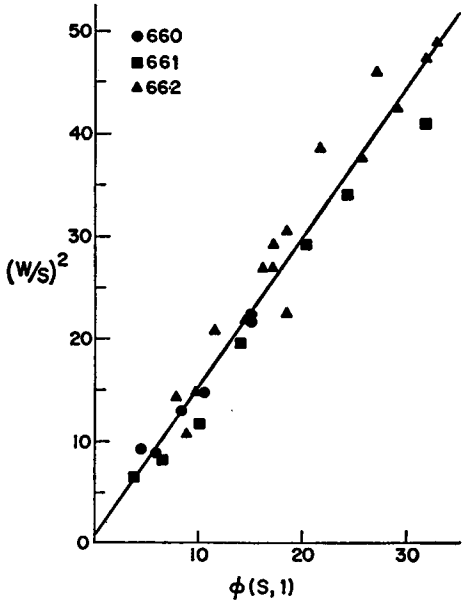

FIGURE 6

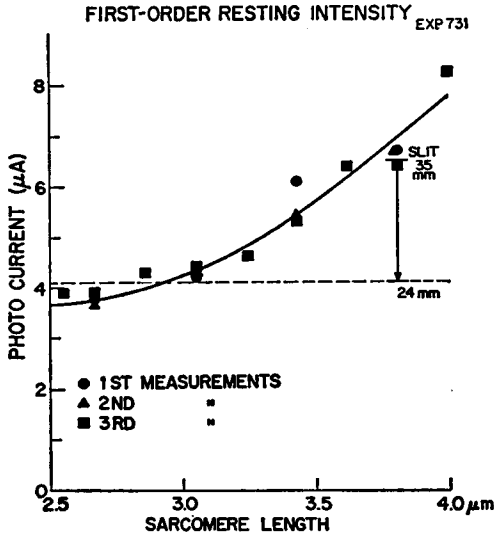

FIGURE 7

FIGURE 6 $(W/S)^2$ vs. $\phi_1(S, l)$ for a bundle of five fibers.

FIGURE 7 First-order diffraction line intensity vs. sarcomere length for resting fiber. Measured with PMT at 40 cm from fiber preparation. A fixed 35 mm slit was placed in front of the PMT. At $S = 3.8$ μm, the slit was narrowed to 24 mm, and the drop of the intensity is indicated by the arrow. The new level corresponds the intensity of 2.6 μm approximately. See text for the meaning of the experiment.

detector, and (*iii*) imperfections of the cylindrical lens and its orientation toward the diffracted beam. These terms do not spread with distance between the sample and the detector, thus making it possible to separate out these terms from the dispersion measurement. The laser beam radius is about 1 mm. Hence, our r value of 1.7–3 mm indicates contributions from terms (*ii*) and (*iii*).

The *intrinsic* dispersion of the sarcomere length when corrected for the above effects is 1–2% in fresh fiber bundle preparation. This means the standard deviation of the sarcomere lengths from their averaged value is only 30 nm, or 15 nm for half-sarcomeres (based on 3 μm sarcomere length and 2% dispersion). The latter number is comparable with the distance between two neighboring cross bridges along the myosin filament (143 Å according to Huxley and Brown, 1967). Therefore it can be said that the lengths of the sarcomeres in frog semitendinosus muscle fibers are highly uniform.

Activation. On isometric tetanic stimulation we did not observe any oscillatory motion of the sarcomere length. Instead we observed a small decrease of the sarcomere length and a small increase of the length dispersion of the sarcomeres. This small contraction (44 nm per sarcomere at most) is thought to be achieved by stretching the passive elements (tendon, transducer, etc.). This hypothesis would predict that the degree of contraction should be directly proportional to the tension development at each sarcomere length. This is not the case in Fig. 4 C. The contraction is maximal when S is 2.5–3.2 μm and decreases at lower and higher sarcomere lengths. The reason for this plateau is not clear, but it may be worthwhile to point out that this plateau level corresponds to one-half of the cross-bridge pitch distance (429 Å according to Huxley and Brown, 1967) around the myosin filament. Since two interaction sites are present in both halves of the A band, relative motion between thick and thin filaments is 22 nm.

The change of the length dispersion on activation decreases monotonically as S increases from 2.2 to 3.6 μm (Fig. 4 D). It is between 20 and 50 nm in the middle sarcomere length range (2.5–3.2 μm). This number is in fact an upper limit of the real change in the dispersion of the sarcomere lengths because background scattering (if any) increases on stimulation and our monitoring system does not subtract this incremental change in scattering. The range of the dispersion change is comparable with the sarcomere length shortening (above). These results suggest that some of the sarcomeres shorten on stimulation whereas some others remain at the initial length. Taylor and Rüdel (1970) observed that the sarcomeres closer to the surface membrane shorten more than those at the core of the muscle fibers, but since the sarcomere length in their preparations is below the slack length ($S \leqq 2$ μm) their results must not be directly comparable. Another interesting explanation is that the relative positions of thick and thin filaments vibrate back and forth asynchronously. If so we would see no vibration in the lengths of sarcomeres (because the motion is asynchronous) but would detect a broadening of the dispersion

of the sarcomere length. The amplitude of such motions, if they exist, must be 44 nm or less. One other possibility, the existence of standing wave, can be excluded because of lack of vibration in the tension record during isometric tetanus. However we emphasize that the most likely possibility is that the length dispersion simply increases as a result of heterogeneous sarcomere shortening.

Addendum

After the present report was reviewed, Cleworth and Edman (1972) published a paper on a similar subject in which they focused on the sarcomere length change. Their observation parallels our observation except for the following point. They failed to detect an increase in the dispersion of the length of the sarcomeres and this contradicts our observation. However as they described it ("the width of the first-order line obtained from a fibre at rest was generally no greater than the diameter of the incident laser beam"), their streak photography technique cannot detect a presence of the 1–2% dispersion of the length of the sarcomeres which we have seen. Since incremental change of the dispersion on stimulation is similar in order of magnitude, it would be impossible to see this change with the streak photography technique.

APPENDIX I

Effect of Finite Size of Laser Beam on Line Width of the Diffraction Patterns

Let $f(S)$ be the intrinsic distribution function of the lengths of the sarcomeres, and assume that $f(S)$ is a gaussian function:

$$f(S) = \exp\left\{-\frac{(S - S_0)^2}{2\sigma^2}\right\}, \tag{4}$$

where S_0 is the average of the sarcomere length, and σ is a spread of the distribution (one-half the length dispersion of the sarcomeres).

Let z be the distance across the laser beam, and $z = 0$ at the center of the beam. It is convenient to express z in the same units as for the sarcomere length change (transformed unit). For example, if δx is a real distance change across a diffraction line, z is related to δx by Eq. 3 when δS is replaced by z. Now let $I(z)$ be the intensity function of the laser beam. Because of the introduction of this function the observed distribution of the sarcomere lengths is modified:

$$F(S) = \int_I I(z)f(S - z)\,dz. \tag{5}$$

The integration is made in the range where $I(z)$ exists. Assume that $I(z)$ is also a gaussian function:

$$I(z) = \exp\{-z^2/2\epsilon^2\}, \tag{6}$$

where ϵ denotes the spread of the laser beam intensity in the transformed unit. Eq. 5 can read-

ily be integrated if we use assumptions 4 and 6:

$$F(S) = (2\pi)^{1/2} \frac{\epsilon\sigma}{(\epsilon^2 + \sigma^2)^{1/2}} \exp\left\{-\frac{(S - S_0)^2}{2\xi^2}\right\}. \quad (7)$$

Eq. 7 tells us how the finite size of the laser beam affects the diffraction patterns, where

$$\xi^2 = \epsilon^2 + \sigma^2, \quad (8)$$

2ξ is the experimentally observed dispersion of the sarcomere lengths. As mentioned above ϵ is related to the radius r of the laser beam by Eq. 3:

$$\epsilon = \frac{(S^2 - n^2\lambda^2)^{3/2}}{Sn\lambda} \frac{r}{l}. \quad (9)$$

We assume that the distribution width is proportional to the sarcomere length:

$$\sigma = \alpha S, \quad (10)$$

α is a proportionality constant. If we define a new function

$$\phi_n(S, l) = \left(\frac{50 \text{ cm}}{l}\right)^2 \frac{(S^2 - n^2\lambda^2)^3}{S^4 n^2 \lambda^2}, \quad (11)$$

then Eq. 8 can be rewritten as

$$(W/S)^2 = a + b \cdot \phi_n(S, l), \quad (12)$$

where

$$a = 4\alpha^2, \quad (13)$$

$$b = (2r/500 \text{ mm})^2. \quad (14)$$

$W, S, \phi_n(S, l)$ are measurable quantities and a plot of $(W/S)^2$ vs. $\phi_n(S, l)$ must yield a linear relationship if Eq. 10 is correct. This appears to be the case when $n = 1$ (Fig. 6). The intercept of the plot corresponds to the intrinsic dispersion of the lengths of the sarcomeres by Eq. 13. The radius of the laser beam r can be calculated from Eq. 14 by measuring the slope of the plot. Results for the intrinsic dispersion of the lengths of the sarcomeres are given in Table I.

It should be emphasized that we are actually separating two types of contributions to the observed dispersion: the first one has the property of increasing with increasing distance between the sample and the detector, whereas the second one does not spread as a function of this distance provided that the incident laser beam is well collimated. The biggest contribution to the first group is the intrinsic dispersion of the lengths of the sarcomeres. The second group includes all kinds of optical artifacts such as the finite size of the laser beam, detector uncertainty (discrete point approximation), imperfections of the cylindrical lens and its orientation with respect to the incident diffraction line, and so on.

APPENDIX II

Intensity of Diffraction Lines

Born and Wolf (1964, p. 402) give the wave function of a one-dimensional object:

$$U(\theta) = U^0 \int_0^L F(y) \exp\left(-\frac{2\pi y \sin \phi}{\lambda} i\right) dy. \quad (15)$$

This formulation can be applied to the diffraction phenomenon by muscle fibers if y is the distance along fiber axis; $F(y)$ is the transmission function of the muscle (related to the refractive index); $L = NS$, the length of the illuminated portion of the muscle fibers; N is the number of illuminated sarcomeres along y axis; S, the sarcomere length; θ, the angular separation from the zero-order reference; and U^0, the amplitude of incident light. Since $F(y)$ is a periodic function it can be expanded in a Fourier series:

$$F(y) = \sum_{n=-\infty}^{\infty} C_n \exp\left[(2\pi n y/S)i\right]. \quad (16)$$

Substituting Eq. 16 into Eq. 15

$$U(\theta) = U^0 \frac{\lambda S i}{2\pi} \sum_{n=-\infty}^{\infty} C_n \frac{\exp\left[(-2\pi L \sin \theta/\lambda)i\right] - 1}{S \sin \theta - n\lambda}. \quad (17)$$

The diffracted light intensity is: $I(\theta) = |U(\theta)|^2$ and $I(\theta)$ has a maximum value, $I^0L^2|C_n|^2$, (I^0 is intensity of the incident light) when

$$S \sin \theta_n = n\lambda. \quad (18)$$

This is the grating equation. The intensity of the nth order diffraction line is the integration of $I(\theta)$ around this maximum:

$$I_n = \int_{n\text{th}} I(\theta)\, d\theta \cong I^0(L\lambda|C_n|^2)/\cos \theta_n. \quad (19)$$

This approximation is valid since the angular separation from the maximum to the first minimum is $\lambda/(L \cos \theta_n)$ which is far less than unity. Thus the nth order intensity is proportional to the wavelength λ, the beam size of laser L, the Fourier coefficient multiplied by its complex conjugate $|C_n|^2$, $1/\cos \theta_n$, and the incident light intensity I^0. The dependence of I_n on sarcomere length comes into the equation only by means of $\cos \theta$ and C_n. Our experiment (Fig. 4) shows that the first-order intensity (I_1) is approximately independent of sarcomere length in resting muscle fibers where S changes from 2.6 to 3.8 μm. This indicates that $|C_1|$ is approximately constant in this sarcomere length range, since the change of $\cos \theta$ is only 2%.

This was supported by the National Institutes of Health grant NS-06614.

We express our thanks and indebtedness to our co-workers in the early phase of this work: W. C. Scott, G. Moran, and G. Purcell.

Received for publication 19 September 1971 and in revised form 10 May 1973.

REFERENCES

APRIL, E. W., P. W. BRANDT, and G. F. ELLIOTT. 1971. *J. Cell Biol.* **51**:72.

BARRY, W. H., and L. D. CARNAY. 1969. *Am. J. Physiol.* **217**:1425.

BORN, M., and E. WOLF. 1964. Principles of Optics. The Macmillan Company, New York. Chap. 8.

BUCHTHAL, F., and G. G. KNAPPEIS. 1940. *Skand. Arch. Physiol.* **83**:281.

CARLSEN, F., G. G. KNAPPEIS, and F. BUCHTHAL. 1961. *J. Biochem. Biophys. Cytol.* **11**:95.

CLEWORTH, D. R., and K. A. P. EDMAN. 1969. *Science (Wash. D. C.).* **163**:296.

CLEWORTH, D. R., and K. A. P. EDMAN. 1972. *J. Physiol. (Lond.).* **227**:1.

COLBY, R. H. 1971. *J. Cell Biol.* **51**:763.

DEWEY, M., K. BLASIE, R. LEVINE, and D. COLFLESH. 1972. *Biophys. Soc. Annu. Meet. Abstr.* **12**:82a.

EBERSTEIN, A., and A. ROSENFALK. 1963. *Acta Physiol. Scand.* **57**:144.

GOLDSPINK, G., R. E. LARSON, and R. E. DAVIES. 1970. *Experimentia (Basel).* **26**:16.

GORDON, A. M., A. F. HUXLEY, and F. J. JULIAN. 1966 *a. J. Physiol. (Lond.).* **184**:143.

GORDON, A. M., A. F. HUXLEY, and F. J. JULIAN. 1966 *b. J. Physiol. (Lond.).* **184**:170.

HILL, D. K. 1949. *J. Physiol. (Lond.).* **108**:292.

HILL, D. K. 1953 *a. J. Physiol. (Lond.).* **119**:489.

HILL, D. K. 1953 *b. J. Physiol. (Lond.).* **119**:501.

HUXLEY, A. F. 1957. *Prog. Biophys. Biophys. Chem.* **7**:255.

HUXLEY, A. F., and L. D. PEACHEY. 1961. *J. Physiol. (Lond.).* **156**:150.

HUXLEY, A. F., and R. M. SIMMONS. 1970. *J. Physiol. (Lond.).* **210**:32P.

HUXLEY, H. E., and W. BROWN. 1967. *J. Mol. Biol.* **30**:383.

KAWAI, M. 1971. Ph.D. Thesis. Princeton University, Princeton, N. J. Chapters 3–6.

LARSON, R. E., M. J. KUSHMERICK, D. H. HAYNES, and R. E. DAVIES. 1968. *Biophys. Soc. Annu. Meet. Abstr.* **8**:A8.

MARIKHIN, V. A., and L. P. MYASNIKOVA. 1970. *Tsitologiya.* **12**:1231.

SANDOW, A. 1936 *a. J. Cell. Comp. Physiol.* **9**:37.

SANDOW, A. 1936 *b. J. Cell. Comp. Physiol.* **9**:55.

TAYLOR, S. R., and R. RÜDEL. 1970. *Science (Wash. D. C.).* **167**:882.